

INGRID: an interactive grid generator for 2D edge plasma modeling

B. M. Garcia,^{1, a)} M. V. Umansky,^{2, b)} J. Watkins,^{3, c)} J. Guterl,^{4, d)} and O. Izacard^{2, e)}

¹⁾*University of California - Santa Cruz, Santa Cruz, California, USA*

²⁾*Lawrence Livermore National Laboratory, Livermore, California, USA*

³⁾*Brigham Young University, Idaho, USA*

⁴⁾*General Atomics, San Diego, California, USA*

(Dated: June 15, 2021)

A fusion boundary-plasma domain is defined by axisymmetric magnetic surfaces where the geometry is often complicated by the presence of one or more X-points; and modeling boundary plasmas usually relies on computational grids that account for the magnetic field geometry. The new grid generator INGRID (Interactive Grid Generator) presented here is a Python-based code for calculating grids for fusion boundary plasma modeling, for a variety of configurations with one or two X-points in the domain. Based on a given geometry of the magnetic field, INGRID first calculates a skeleton grid which consists of a small number of quadrilateral patches; then it puts a subgrid on each of the patches, and joins them in a global grid. This domain partitioning strategy makes possible a uniform treatment of various configurations with one or two X-points in the domain. This includes single-null, double-null, and other configurations with two X-points in the domain. The INGRID design allows generating grids either interactively, via a parameter-file driven GUI, or using a non-interactive script-controlled workflow. Results of testing demonstrate that INGRID is a flexible, robust, and user-friendly grid-generation tool for fusion boundary-plasma modeling.

^{a)}Electronic mail: bgarci26@ucsc.edu

^{b)}Electronic mail: umansky1@llnl.gov

^{c)}Electronic mail: joeymwatkins@gmail.com

^{d)}Electronic mail: guterlj@fusion.gat.com

^{e)}Electronic mail: izacard1@llnl.gov

I. INTRODUCTION

A. Tokamak edge plasma modeling

Research in tokamak edge plasma physics is critical for realizing practical fusion energy and designing future fusion reactors. One of the greatest challenges that tokamak edge plasma researchers face today is determining effective methods for controlling particle and heat fluxes on tokamak plasma-facing components (PFC) while maintaining good core-plasma performance. A possible solution is the use of advanced divertor configurations¹.

The traditional X-point divertor configuration uses a first-order null point for the poloidal field, which is usually placed at the bottom of the core plasma, or at the top. The traditional double-null configuration uses one first-order X-point at the bottom and one at the top.

In contrast, several advanced divertor configurations have been proposed where a secondary X-point is included in the divertor region. These include snowflake-like configurations and the X-point Target configuration. Snowflake-like configurations approximate a configuration with an exact second-order null of the poloidal field dubbed “snowflake”². In practice, instead of an exact second-order null, a configuration is used where two regular X-points are brought close together, which leads to snowflake-plus and snowflake-minus configurations³. On the other hand, for an X-Point Target configuration⁴, a secondary X-point is introduced in the divertor far away from the primary X-point, in the divertor leg near the target plate.

Each of these divertor configuration is characterized by locations of the primary and secondary X-points in the domain. The primary X-point is the most significant as it separates the plasma into the hot core region and colder scrape-off layer (SOL) region. However, a secondary X-point helps redirect and distribute the flux of plasma particles and energy over multiple locations (strike points) on the material surface. Furthermore, a secondary X-point may help increase plasma radiation in the divertor, and potentially it may cause other interesting and important effects in divertor plasma.

B. Grid generation for tokamak edge plasma transport simulations

Tokamak boundary and divertor plasma modeling relies heavily on edge transport modeling codes such as UEDGE⁵, SOLPS⁶, EDGE2D⁷, just to mention a few major ones. These codes are similar in many ways; they all solve the time-evolution fluid equations for toroidally-symmetric, collisional plasma based on the Braginskii equations, using ad-hoc radial transport coefficients.

The simulations are usually carried out in the actual geometry of a modeled tokamak, to account for details of magnetic field geometry and plasma-facing components.

Computational grids for tokamak boundary plasma transport modeling are usually chosen to follow the magnetic flux surfaces, to avoid numerical pollution caused by the extreme anisotropy of plasma transport along and across the magnetic field⁸. Thus the computational grid has to follow the underlying magnetic field, and with one or several X-points present in the simulation domain the grid topology can become highly nontrivial.

There are several grid generators for tokamak edge plasma region currently in use. Among those, the UEDGE code uses a grid generator that is a part of the UEDGE package, SOLPS normally uses grid generator CARRE⁹, and EDGE2D usually relies on grid generator GRID2D¹⁰. These are sufficient in most cases for modeling single-null and double-null configurations. However modeling of advanced divertors may require incorporating secondary X-points in the divertor region, and grid generators currently in use for the major edge transport codes are not inherently designed to produce computational grids for general configurations containing more than one X-point at arbitrary locations in the domain.

To increment the capabilities for grid generation for tokamak boundary plasma transport modeling, in particular for advanced divertors, a new grid generator INGRID has been developed, as described in the present report. INGRID (Interactive Grid Generator) is a Python based, interactive, grid generator for edge plasma transport modeling that is capable of handling configurations with one or two X-points anywhere in the computational domain. INGRID provides a robust set of tools such as an easy to use GUI intended for users of all levels. By internally handling the challenges that typically arise with generating grids for tokamak edge plasma region, INGRID can indeed improve efficiency in a user's workflow for edge-plasma modeling. The INGRID algorithm's inspiration was drawn from an older IDL-based project Gingred¹¹ where a "divide and conquer", domain partitioning approach for grid generation was first tried. An important motivating factor for implementing INGRID in Python was using an open-source language with advanced numerical and graphical libraries.

C. Paper outline

The aim of this current section is to provide a short introduction to tokamak edge plasma modeling, the state of grid generation for tokamak edge plasma simulations, and motivate the develop-

ment of INGRID. The next section discusses the classification of equilibria found within a plasma device. Here we define the magnetic topologies that INGRID has been designed to model. Following our discussion on classification, we elaborate on the computational methodology INGRID adopts. Here the interpolation scheme, topology analysis, Patch map construction, and grid construction is detailed. Following our computational algorithm discussion, a benchmark of INGRID is presented. This discussion then leads us into our section on software design. The INGRID package structure, classes, and data formats are discussed. Finally, we summarize our results and point the reader to where INGRID can be obtained.

II. CLASSIFICATION OF EQUILIBRIA

The geometry of a tokamak (or a similar toroidal plasma device, like a spheromak or a reversed-field pinch) is defined by the flux function $\Psi(R, Z)$ such that $\nabla\Psi \cdot \vec{B} = 0^{12}$. Then the poloidal magnetic field components B_R, B_Z can be expressed as

$$B_R = -\frac{1}{R} \frac{\partial\Psi}{\partial Z} \quad (1)$$

$$B_Z = \frac{1}{R} \frac{\partial\Psi}{\partial R} \quad (2)$$

$$(3)$$

Surfaces $\Psi(R, Z)=\text{const}$ form a set of nested magnetic flux surfaces confining the plasma, and the magnetic field is tangential to the flux surfaces. The nulls of the poloidal magnetic field, $B_R = B_Z = 0$ correspond to extrema or saddle points of the flux function $\Psi(R, Z)$. The “magnetic axis” corresponds to an extremum of Ψ at the innermost flux surface. Further we consider first-order saddle points of Ψ where its first derivatives vanish, those points are “X-points”.

To understand the range of geometric possibilities in presence of one and two X-points in the domain, consider the diagrams in Fig.(1). If there is a single X-point in the region it defines a separatrix which is a flux surface containing the X-point Fig. (1 (a)). The X-point is a self-intersection point of the separatrix that divides the plane into three topologically distinct regions. One is the “core plasma region”, containing the magnetic axis. Next, there is a region lying opposite to the core plasma region, across the X-point, and it is called the “private flux region”, or PFR. And the remaining part is the “common flux region”, or scrape-off-layer (SOL) region.

A second X-point can be added outside of the core plasma region. Ignoring the degenerate case when the secondary X-point is on the primary-separatrix, there are two topologically distinct possibilities: with respect to the primary separatrix the second X-point can be either in the private flux region, Fig. (1 (c)); or in the common flux region Fig. (1 (b)). The former case is called “snowflake-plus” and the latter case is called “snowflake-minus”².

However, from the grid generation perspective, we consider further variations of “snowflake-like” configurations, as shown in Fig. (1). Consider a line orthogonal to flux surfaces and passing through the secondary X-point X_2 , and consider the intersection of this line with the primary separatrix, X'_2 . For “snowflake-minus” configuration there five possibilities for the projection point X'_2 . It can belong to: (i) the arc $[M_W, M_E]$ connecting the two midplane-level points, or (ii) the arc $[M_W, X_1]$, or (iii) the arc $[M_E, X_1]$, or the arc (iv) $[X_1, S_W]$ connecting the primary X-point and one of the “strike-points”, or (v) the arc $[X_1, S_E]$. For “snowflake-plus” configuration, there are two possibilities for the projection point X'_2 . It can belong to: (i) $[X_1, S_E]$, or to (ii) $[X_1, S_W]$.

Based on the location of the secondary X-point X_2 and its orthogonal projection on the primary separatrix X'_2 , we use the following notation for the configurations with two X-points:

- UDN: $SF-, X'_2 \in [M_E, M_W]$
- SF15: $SF-, X'_2 \in [M_E, X_1]$
- SF165: $SF-, X'_2 \in [M_W, X_1]$
- SF45: $SF-, X'_2 \in [S_E, X_1]$
- SF135: $SF-, X'_2 \in [S_W, X_1]$
- SF75: $SF+, X'_2 \in [S_E, X_1]$
- SF105: $SF+, X'_2 \in [S_W, X_1]$

The orthogonal projection and magnetic configurations mentioned above are seen in figs. (1, 2-9). The notation for snowflake-like configurations is inspired by local geometric analysis of near-snowflake configurations and the numbers correspond to the geometric angle defining the position of the secondary X-point¹³. Our geometric classification here is topology-based, it applies to more general situations when the two X-points can be far apart; but the notation introduced in literature¹³ is still useful. All in all, with the single-null (SNL) configuration included, for either

one and two X-points in the domain, there are eight possible configurations. We do not consider here degenerate cases where the secondary X-point is exactly on the primary separatrix, or the projected point X'_2 is exactly on the primary X-point X_1 , or it is exactly on a midplane point M_E or M_W ; the assumption is that a practical, experiment-relevant configuration would always have some finite degree of asymmetry to fall into one of the eight considered categories.

III. COMPUTATIONAL ALGORITHM METHODOLOGY

A. Domain partitioning strategy

The INGRID workflow includes two main steps: (i) constructing a “skeleton grid” (also called further a “Patch-Map”) which corresponds to the geometry of the magnetic field in hand and consists of a small number of quadrilateral patches; and (ii) putting a subgrid on each of the patches. This is illustrated in Fig. (10) where a Patch-Map is shown with one of the patches covered with a subgrid.

The skeleton grid is constructed as a small grid aligned with the given poloidal magnetic field and respecting the magnetic field topology. The geometry of magnetic flux surfaces, in particular the X-points and the magnetic axis, and the geometry of plasma facing material surfaces all together define a patch map. For calculating a subgrid, the code divides each quadrilateral patch into a number of radial and poloidal zones according to user-provided input. Finally, all subgrids are joined together to produce the global grid.

B. Magnetic field interpolation

Input data for grid generation come in the form of the poloidal magnetic flux Ψ sampled on rectangular grid in R, Z , from an MHD reconstruction code such as EFIT¹⁴ or TEQ. INGRID utilizes a bicubic interpolation implementation¹⁵ for obtaining the values of the poloidal magnetic flux Ψ and its derivatives between data points of a provided magnetic equilibrium. This functionality is provided by class `RectBivariateSpline` belonging to the `scipy.interpolate`^{16,17} package.

Poloidal flux surfaces are reconstructed in INGRID by integrating the ODEs,

$$\dot{R} = -\frac{1}{R} \frac{\partial \Psi}{\partial Z} \quad (4)$$

$$\dot{Z} = \frac{1}{R} \frac{\partial \Psi}{\partial R} \quad (5)$$

whereas surfaces orthogonal to poloidal flux surfaces are reconstructed by integrating the ODES,

$$\dot{R} = \frac{1}{R} \frac{\partial \Psi}{\partial R} \quad (6)$$

$$\dot{Z} = \frac{1}{R} \frac{\partial \Psi}{\partial Z} \quad (7)$$

The bicubic interpolation guarantees continuity of first derivatives of Ψ at the edges of cells of the original R, Z grid, so the resulting flux surfaces are smooth.

C. Calculation of reference points

The topology of magnetic flux surfaces in tokamak edge plasma is defined by relative positions of X-points and the magnetic axis. These key reference points are calculated in INGRID by finding nulls of the poloidal field, solving the equation

$$\left(\frac{\partial \Psi}{\partial R}\right)^2 + \left(\frac{\partial \Psi}{\partial Z}\right)^2 = 0 \quad (8)$$

INGRID utilizes method `scipy.optimize.root`^{16,18} for this purpose. For finding the correct root of this equation the solver needs an accurate initial guess; the user is supposed to provide initial guess for the magnetic axis and for one or two of those X-points that are expected to be included in the domain.

D. Topology analysis

INGRID performs topology analysis and classification based on the user specification of one or two X-points in the domain. We first consider when only one X-point is to be analyzed. The tokamak edge plasma community often classifies single X-point configurations as “upper single

null” or “lower single null.” However, for INGRID there is no distinction. If one X-point is specified, then INGRID considers the aforementioned configurations as a general single-null (SNL) configuration. Instead of using “lower” and “upper” for the divertor, and “inner” and “outer” for target plates, INGRID uses compass directions North-South-East-West associated with the primary X-point. The North direction is defined to point into the core plasma along the $\nabla\Psi$ direction, whereas the South direction is defined to point into the private-flux along the $\nabla\Psi$ direction. East and West are then defined orthogonal to the North and South directions. For example, the inner target plate of an LSN configuration is in the south-west direction of an SNL configuration, as illustrated in Fig. (2). Similarly, the inner target plate of a USN configuration is in the south-east direction. Determining the North-South-East-West directions associated with the primary X-point is the extent of the analysis performed in the SNL case.

If two X-points in the domain are to be analyzed, INGRID performs additional analysis to determine the specific magnetic topology. INGRID begins by performing the compass analysis from the SNL case on the primary X-point. Next, INGRID determines whether the secondary X-point is in the private-flux (PF) region or in the common-flux region (SOL) with respect to the primary separatrix. If the secondary X-point resides in the private-flux, the configuration is of type SF+. If not, the configuration is of type SF-. This determination is conducted by representing the PF as a generalized polygon and determining whether a 2D point representing the X-point is contained within the polygon or not. The vertices of the polygon correspond to the points obtained from the portion of the limiter contained between points S_W and S_E (denoted as $[S_W, S_E]$) and line tracing (detailed in section E) the two arcs $[X_1, S_W]$, $[X_1, S_E]$. INGRID implements the point-in-polygon test with the help of class `matplotlib.path`. Representing the polygon boundary as a `matplotlib.path` object, the method `matplotlib.path.contains_point` can then determine whether the area enclosed by the path contains the given point or not. With the point-in-polygon test completed, an orthogonal projection is constructed from the secondary X-point to the primary separatrix. This is done by line tracing equations (3) and (4) where the termination criteria is intersection with the primary separatrix. Finally, the specific magnetic topology is determined by the criteria outlined in Section II for classification of equilibria.

E. Patch-Map construction

After the analysis of magnetic geometry for a given magnetic field and establishing what configuration corresponds to it, INGRID creates a corresponding Patch-Map which is an ordered collection of quadrilateral patches defining the skeleton grid. A Patch-Map is a 2D array of patches where one index corresponds to the radial direction, and the second index corresponds to the poloidal direction; thus the order of patches in a Patch-Map defines what patches are neighbors of a given patch in the radial and poloidal directions.

A Patch-Map is constructed using numerical integration and line tracing of poloidal and radial surfaces through the X-points, and radial and poloidal surfaces defining the domain boundaries. INGRID utilizes the method `solve_ivp` from the `scipy.integrate`¹⁶ package for all numerical integration purposes. In particular, LSODA¹⁹ was selected as the `solve_ivp` method of integration. Equations (1) and (2) provide INGRID the capability to reconstruct poloidal flux, whereas equations (3) and (4) provide INGRID the capability to reconstruct radial flux surfaces. The process of flux surface reconstruction and, when applicable, visualization of the reconstruction we refer to as line tracing. Radial domain boundaries are flux surfaces corresponding to maximum and minimum values of the poloidal flux function Ψ , these values are defined by the user in the input file. The poloidal domain boundaries are target plates surfaces, also defined in the input file. For each of the divertor configurations that INGRID can use - which includes a single-null, unbalanced double-null, and six snowflake-like configurations - there is a specific type of Patch-Map that defines the topology of this configuration. For example, for a SNL configuration shown in Fig. (2), a Patch-Map includes two radial zones, two poloidal zones defining divertor legs, and four poloidal zones defining the edge plasma domain around the last closed flux surface. Such a Patch-Map that contains twelve patches is sufficient to represent a general single-null geometry, albeit in a most basic and crude way. Note that one could use only ten patches to represent the single-null topology, but using twelve patches allows matching more accurately the general shape of a single-null configuration. Furthermore, a finer grid representing a single-null geometry can be always represented as this Patch-Map with local refinement applied to one or several of these twelve patches. For a more complicated unbalanced double null (UDN) geometry shown in Fig. (3), the Patch-Map must include three radial zones because there are two separatrices there. There are four poloidal zones to represent four divertor legs there, and together with four poloidal zones covering the core domain there are total eight poloidal zones. All in all, there are twenty four

patches in this case. Similarly, for each of the snowflake-like configurations there are twenty four patches, as illustrated in Figs. (4-9). It is important to comment on the consistency of boundaries of each Patch with adjacent Patches. Regardless of divertor configuration, each Patch map generation method enforces that boundaries align radially by simply defining adjacent Patch boundaries in terms of the same boundary. Poloidal consistency of Patch boundaries along the north and south is attained by simply continuing line tracing from the end point of the adjacent Patch. It should be noted that this process cannot guarantee the consistency of Patch boundaries along the upper core. This boundary mismatch, however, is directly related to line tracing tolerance and can be controlled by the `tol` attribute found within the integrator settings of the parameter file.

F. Grid construction

For a given magnetic configuration, a Patch-Map represents a very crude grid where each Patch is a “quadrilateral” with four vertices. The radial sides of this quadrilateral are defined by two flux surfaces, $\Psi(R,Z) = \Psi_1$ and $\Psi(R,Z) = \Psi_2$. The poloidal sides of a Patch are usually constructed to be aligned with $\nabla\Psi$, which makes the skeleton grid locally orthogonal.

However, more generally the poloidal sides of a Patch can deviate from the $\nabla\Psi$ direction. For example, for those patches that contain the poloidal boundaries of the domain, given by the target plates, one of the sides is defined by the target plate shape. The curve describing the target plate can be arbitrary, as long as it does not form “shadow regions”, i.e., Ψ is a monotonic function of the length along the plate.

Going beyond the skeleton grid, a Patch can be divided in a number of radial and poloidal zones, forming a subgrid local to this patch. The radial zones are constructed to be aligned with flux surfaces, so the global grid remains aligned with the poloidal magnetic field. For the poloidal zones, the main algorithm is based on dividing the patch poloidally into uniform length line segments. However, as described further, there are options in the code for controlling the radial and poloidal distribution of subgrid.

The radial and poloidal dimensions and distribution of subgrid on a given Patch are not entirely independent of subgrids on other patches as the global grid still has to be Cartesian in the index space. Thus the poloidal grid has to be consistent for those patches that are stacked on top of each other radially, and the radial grids have to be consistent for those patches stacked on top of each other poloidally.

G. Grid customization

INGRID provides users a number of tools for customization of generated grids, which can be controlled via the parameter file. Users can modify both the Patch-Map and the subgrids in order to optimize the global grid.

Default settings for constructing a Patch-Map use the horizontal plane through the magnetic axis, commonly referred to as the midplane. For grid generation purposes, INGRID allows shifting the effective magnetic axis location vertically and horizontally. Moreover, instead of using the horizontal directions for the midplane, the user can set two angles defining a “generalized midplane”. Since the midplane can be thought of as two rays emanating from the magnetic axis with angles 0 and π radians, the “generalized midplane” is defined similarly but with user-defined “effective magnetic axis” location, and with user-specified angles for both rays.

Also, for those patches that include an X-point as one of their vertices, the default poloidal boundaries use in the East and West directions from the X-point along the $\nabla\Psi$ direction. However, the user can redefine those curved, replacing them by straight lines in a desired direction.

For fine-tuning the grid, subgrids can be adjusted as well. By default, during Patch refinement, grid seed-points are distributed uniformly in length along the radial boundaries and distributed uniformly along the poloidal boundaries in locally-normalized Ψ . This default behavior can be changed so that grid seed-point placement obeys a user specified distribution function.

Another important customization feature in INGRID is a “distortion_correction” tool for mitigating grid shearing. This tool allows the user to bound the angles found within the interior of a grid cell in order to generate nearly orthogonal subgrids in patches. The implementation is as follows. Let a quadrilateral cell of a subgrid be defined by four nodes A, B, C , and D where AB is the top-face, BC is the right-face, CD is the bottom-face, and DA is the left-face of the cell. The angle $\angle DAB := \alpha$ is measured. If α is not within a user-defined range $[\alpha_{\min}, \alpha_{\max}]$, then the node D is translated along the poloidal flux surface until α is within the range. The direction of translation is determined by whether $\alpha \geq \alpha_{\max}$ or $\alpha \leq \alpha_{\min}$. During the translation of D , we must also avoid collision with a neighboring node on the poloidal flux surface. To ensure collision does not occur, the translation stops when the moving node D comes within ε of a neighboring node. Upon termination, the current value of α is used to define the transformed cell. An example of the distortion_correction feature applied to a grid can be seen in Fig.(11).

IV. PERFORMANCE

A. Scaling of calculation time

The results of INGRID timing test are shown in Table (I) and in Fig. (12). These tests were run on an Apple Mac Mini (2020 model) housing an Apple M1 chip (3.2 GHz processor). The scaling appears sublinear for small grids; for larger grids it asymptotes to linear. Note that the cost of grid generation is not significant in a typical edge plasma modeling workflow; running the simulation takes orders of magnitude more computing time. This scaling makes INGRID practical for constructing large grids.

SNL			SF75		
Cells Per Patch	Total Cells	Time (s)	Cells Per Patch	Total Cells	Time (s)
9	108	8.02	9	243	21.32
16	192	11.44	16	432	27.69
25	300	14.79	25	675	34.45
36	432	18.29	36	972	41.10
49	588	21.58	49	1323	48.31
64	768	25.02	64	1728	54.82
81	972	28.49	81	2187	62.24
100	1200	32.27	100	2700	68.69
121	1452	35.32	121	3267	75.44
144	1728	38.61	144	3888	82.63
169	2028	41.98	169	4563	89.97
196	2352	45.46	196	5292	96.21
225	2700	49.08	225	6075	103.71

Table I: A benchmark of grid generation for both an SNL and SF75 configuration. Grids were generated with $n \times n$ many cells per Patch with $n = \{3, 4, 5, \dots, 15\}$. With $n \times n$ subgrid dimensions, SNL configurations contain $12n^2$ many cells, whereas SF75 configurations contain $27n^2$ many cells.

B. Benchmark testing

To verify grids calculated by INGRID, several benchmark tests have been performed with the UEDGE code.

In these testes, UEDGE solutions were compared, using grids from INGRID and grids produced with the UEDGE internal grid generator; for the same physics problem statement, the same boundary conditions, using the same (or very close) domain geometry.

In one of these test problems, a snowflake-like SF75 configuration was used, based on magnetic reconstruction data from the TCV tokamak. The UEDGE grid generator cannot deal with the SF75 configuration directly; but it can be set up to treat each X-point as a part of a separate SN configuration, and then joining two such SN grids together one can produce a grid for the full SF75 domain.

The UEDGE code was set up to solve to the steady state the time-evolution equations for plasma density, plasma parallel momentum, ion thermal energy, and electron thermal energy.

$$\frac{\partial}{\partial t} n_i + \nabla \cdot [n_i \vec{V}_i] = S_i \quad (9)$$

$$\frac{\partial}{\partial t} [M n_i V_{i,\parallel}] + \nabla \cdot [M n_i \vec{V}_i V_{i,\parallel} - \hat{\eta}_i \nabla V_{i,\parallel}] = S_{m,\parallel} \quad (10)$$

$$\frac{\partial}{\partial t} \left[\frac{3}{2} n T_i \right] + \nabla \cdot \left[\frac{5}{2} n_i T_i \vec{V}_i + \vec{q}_i \right] = S_{E,i} \quad (11)$$

$$\frac{\partial}{\partial t} \left[\frac{3}{2} n T_e \right] + \nabla \cdot \left[\frac{5}{2} n_e T_e \vec{V}_e + \vec{q}_e \right] = S_{E,e} \quad (12)$$

Here we use the standard notation: n_i is the plasma density, \vec{V}_i is the plasma fluid velocity, $T_{e,i}$ is the electron and ion temperature, $\vec{q}_{e,i}$ is the electron and ion heat flux, S_i , $S_{m,\parallel}$, $S_{E,e,i}$ are sources of plasma density, parallel momentum, and electron and ion thermal energy⁵.

The grids used for the calculation are shown in Fig. (13). The grid generated with the UEDGE grid generator is constructed to be strictly locally orthogonal; the grid from INGRID is not orthogonal. Also, there is slight difference in the domain shape; the grid from INGRID uses flat target plates while the grid from UEDGE uses curved target plates orthogonal to Ψ . Still, the steady state solutions exhibit essentially the same distributions of plasma density, temperature, and parallel flow velocity, as can be seen in Fig. (14). Beyond that, a quantitative comparison of radial

plasma profiles at the outer midplane was carried out, with reassuring results indicating absence of any major issue in INGRID grids.

V. SOFTWARE DESIGN AND USER INTERACTION

A. INGRID package

INGRID has been exclusively developed in the Python programming language to take advantage of the free, community supported graphical and numerical libraries, and due to the increasing popularity in major tokamak plasma modeling projects such as OMFIT^{20,21} and PyUEDGE²². The `Ingrid` class contained within the `ingrid` module provides the primary API for users. This `Ingrid` class is used to activate INGRID's GUI mode and also contains high-level methods for importing data, visualizing data, analyzing data, grid-generation, and exporting of data; all of which can be utilized noninteractively in Python scripts. Class `IngridUtils` is contained within the `utils` module and serves as the base class for `Ingrid`. `IngridUtils` class methods encapsulate much of the lower-level software details used to implement the methods in the `Ingrid` class. Because of this, `IngridUtils` is encouraged for use by advanced users and developers of INGRID. In addition to `IngridUtils`, class `TopologyUtils` can be found within the `utils` module. In a manner similar to `IngridUtils`, the `TopologyUtils` class serves as a base class for each magnetic-topology class within the `topologies` subpackage. `TopologyUtils` contains key methods for generating Patch-Maps, visualizing data, generating grids, and exporting grids in `gridue` format. Eight magnetic-topology classes are contained within their own modules within the `topologies` subpackage: `SNL`, `UDN`, `SF15`, `SF45`, `SF75`, `SF105`, `SF135`, and `SF165`. Each magnetic-topology class contains configuration specific line-tracing instructions for construction of Patch-Maps, Patch-Map layout information, and `gridue` formatting information. `Ingrid` and `IngridUtils` conduct analysis of MHD equilibrium data in order to decide which magnetic-topology class to instantiate from the `topologies` subpackage. The `IngridUtils` class always maintains a reference to the instantiated object in order to effectively manage grid-generation.

All GUI operation is managed by class `ingrid_gui` within the `guis` subpackage. INGRID's GUI front-end was developed with the Tkinter package; a Python interface to the Tk GUI toolkit that is available within the Python Standard Library. Class `ingrid_gui` is simply responsible for managing event handling, and managing an `Ingrid` object that is used to drive the GUI with direct

calls to the available high-level methods.

Beyond modules `ingrid` and `utils`, modules `geometry`, `interpol`, and `line_tracing` form the computation and modeling foundation of INGRID. Class `EfitData` can be found within the `interpol` module. Class `EfitData` is used to provide an interpolated representation of provided MHD equilibrium data. `EfitData` computes partial derivative information of MHD equilibrium data, provides interpolated Ψ function values by interfacing with class `scipy.interpolate.RectBivariateSpline`, and contains methods for visualisation of interpolated MHD equilibrium data. Module `geometry` contains classes `Point`, `Line`, `Patch`, and `Cell`. These classes are the building-blocks for creation of Patch-Maps and generation of grids.

B. INGRID geometry object hierarchy

If we are to adopt an object-oriented approach to grid generation, then we must develop a set of tools that can be utilized throughout our project. Here we discuss how INGRID defines a collection of geometric classes in order to make the grid generating process as simple as possible for all magnetic topologies of interest. To do so, INGRID defines the following collection of geometric abstractions: the `Point` class, the `Line` class, the `Cell` class, and the `Patch` class. All together, these classes arm INGRID with the ability to represent any magnetic topology of interest. We provide a very brief description of the classes here. Figure 10 illustrates the geometry collection described below. A `Point` object simply represents an arbitrary (R, Z) spatial coordinate in the computational domain. Along with (R, Z) , coordinates, Ψ values can be returned from the `Point` object. A `Line` object is defined by a list of two or more `Point` objects. This `Line` object definition allows for the representation of any arbitrary curve we may encounter (e.g. constant Ψ surface, target plate, limiter geometry). This can be done since the collection of `Point` objects correspond to segments that are the discretization of the curve of interest. A `Patch` object represents a closed region of the domain, and a block of the block-structured mesh INGRID computes. Patches are defined by four `Line` objects. The “North” `Line` (top), “East” `Line` (right), “South” `Line` (bottom), and “West” `Line` (left) define the `Patch` borders which form a closed, clockwise-oriented loop. Methods of the `Patch` class assist with visualization and computation. For example, `Patch` method `make_subgrid` directly handles grid generation for the local region of interest. A `Cell` object resides within a `Patch` and represents a quadrilateral grid cell. Cells are defined by five `Point` objects: four corners (NW, NE, SW, SE) and a center. These `Cell` objects provide the spatial and experimental data that

are written to exported grid files.

From these definitions, we have the building blocks for modeling any of the magnetic topologies of interest we mentioned in the previous section. In particular, we aim to construct a collection of Patch objects representing the divertor configuration of interest. We call this collection of Patch objects a Patch-Map. This Patch-Map allows us to create a grid of Cell objects within each Patch, thus providing the final grid. The management of the Patch-Map creation and grid generation is managed by a magnetic topology class of modeling interest. As of the current INGRID release, we have defined magnetic topology classes SNL, UDN, SF15, SF45, SF75, SF105, SF135, and SF165. These are contained within a dedicated topologies subpackage within the INGRID code.

C. INGRID parameter file

We have decided to use YAML formatted files for the parameter file²³ for user control INGRID in GUI mode and restoring sessions in non-interactive scripting mode. This YAML file is similar to the familiar Fortran namelist files due to the key-value structure it employs. YAML is in an easy to read format that has extensive support within Python. With the PyYAML library, Python reads a YAML formatted file and internally represents it as a Python dictionary. This allows users to model cases in the INGRID GUI and reuse a parameter file in scripting for later usage (e.g. batch grid generation). Some key controls within the parameter file include: EFIT file specification, specification of number of X-points, approximate coordinates of X-point(s) of interest, approximate magnetic-axis coordinates, Ψ level values, and target plate settings (files, transformations). Other controls in the parameter file include: path specification for data files, grid cell np/nr values, poloidal and radial grid transformation settings, limiter specific settings, saving/loading of Patch maps, gridue settings, and debug settings. This is not an exhaustive list. Further details can be found in INGRID's Read The Docs online documentation.

D. INGRID target plate file

INGRID users must specify the geometry of the limiter and/or target plates (by which we mean here the entire first-wall contour surrounding the plasma), to represent the shape of material walls in a modeled device. The limiter and target plates are represented in INGRID by a piecewise-linear model defined by a set of nodes; the (R,Z) coordinates of those nodes are expected to be provided

in separate data files. There is one data file for the limiter and one for each target plate, either in the text format or as a NumPy binary. The names of those data files are set in the INGRID parameter file. In the case that the limiter and target plate data are provided in text format, the user must specify the (R,Z) coordinates for each point defining the surface sequentially on a separate line in the corresponding data file; and Python-formatted single-line comments can be included, as shown in the Appendix.

For use of NumPy binary files, users must also adhere to a particular internal file structure. Given two NumPy arrays of shape $(n,)$ that represent R and Z coordinate values respectively, one can define a NumPy array of shape $(2,n)$ representing the n -many points required to model the piecewise-linear model of interest. This NumPy array of shape $(2,n)$ can be saved into a NumPy binary file in order to be loaded into INGRID. In addition to the requirements above, INGRID asserts that strike-point geometry files used for Patch-Maps are monotonic in Ψ along the length of the target plates (i.e. no shadow regions). The requirement of target plates to be monotonic in Ψ allows INGRID to parameterize the (r,z) coordinates of the geometry with the Ψ values. With a unique mapping of Ψ to (r,z) target plate coordinates, INGRID can generate Patch objects that conform exactly to the plate or limiter geometry. While operating INGRID in GUI mode, users will be warned if the loaded geometry file is not monotonic in Ψ along the target plate length.

E. INGRID workflow

INGRID can be operated via GUI or utilizing the INGRID library directly in Python scripts. The GUI workflow highlights the interactive nature of INGRID by allowing users to visually inspect MHD equilibrium data, configure geometry, and refine parameter file values on the fly. Figure 15 shows the simple GUI with both MHD equilibrium data, and the corresponding grid plotted (text editor not pictured, see Appendix for parameter file). For both GUI operation and scripting with INGRID, the high-level INGRID workflow is: (i) Parameter file visualization and editing, (ii) Analysis of MHD equilibrium data and creation of Patch-Map, (iii) Patch-Map refinement and grid export.

INGRID internally handles step (ii) and leaves the user to with steps (i) and (iii). These steps are where the user is able to customize the Patch-Map and grid to meet their modeling needs.

Step (i) in the INGRID workflow allows users to visually inspect MHD equilibrium data, target-plates and limiter geometry, and Ψ -level contours that are specified within a loaded parameter file.

Since creation of grids is tied directly to MHD equilibrium analysis and Patch-Map creation, step (i) is crucial for successful grid generation. To simplify this step, the INGRID GUI provides an easy to use environment for preparation of a parameter file for the subsequent analysis of MHD equilibrium data and Patch-Map creation. Examples of common operations at this step include modifications to strike-point geometry and Ψ -level boundaries for subsequent Patch-Maps. Once a user is satisfied with parameter file settings, step (ii) can be immediately executed with no further user intervention. Should any errors in Patch-Map creation occur (e.g. misplaced target-plates, Ψ -boundaries that do not conform to configuration specific requirements), INGRID will prompt the user and allow for appropriate edits to be made. Upon completion of step (ii), the created Patch-Map will be provided to users as a new matplotlib figure. From here the user can decide to proceed with Patch-Map refinement or start over at step (i) to make edits to the Patch-Map.

In order to streamline grid generation and skip directly to step (iii), INGRID supports Patch-Map reconstruction. This feature allows users to bypass line-tracing routines by reloading a saved Patch-Map from a previous INGRID session. To do so, INGRID encodes essential geometry and topology analysis data in a specially formatted dictionary that is then saved as a NumPy binary file. Class `IngridUtils` handles the encoding and reconstruction of Patch-Maps. These reconstruction features can be configured by the user within the INGRID parameter file.

After a Patch-Map has been generated or reconstructed, users can configure grid generation specific settings that will be utilized during Patch-Map refinement. Similar to Patch-Map generation, once all local subgrids have been created within Patch objects, a new matplotlib figure is presented with the generated grid. From here, users can make grid generation setting edits in the INGRID parameter file or proceed to exporting a gridue file.

VI. SUMMARY

INGRID is a new grid generator for tokamak boundary region, it is capable of producing grids for single-null (SNL), unbalanced double-null (UDN), and snowflake-like (SF) configurations. Currently, exported grids are in the format of the UEDGE code, as detailed in Ref. ⁽²⁴⁾; future development may include addition of grid formats used by other codes if INGRID is adopted in the broader edge-plasma community, beyond UEDGE. INGRID can be utilized via the INGRID Python package, or through a parameter file driven GUI mode. Source code as well as documentation is publicly available on GitHub²⁵ and Read the Docs²⁶ respectively. The internal equilibrium

topology analysis algorithm provides the ability to automatically identify the divertor configuration embedded within experimental data with minimal user interaction. The geometry class hierarchy approach to domain partitioning and Patch-Map abstraction is an essential component of INGRID and results in a modular approach to grid generation. These localized grids are combined into a global grid that are then ready for export. Current computational scaling of grid generation algorithm follows a sublinear trend independent of magnetic-topology modeled. Benchmarking of INGRID against the internal grid generator in UEDGE is demonstrated for an SF75 snowflake-like configuration. These tests illustrate INGRID’s ability to produce practical grids for tokamak edge modeling, for complex magnetic flux function with one or two X-points in the domain, and for nontrivial target plate geometry.

VII. ACKNOWLEDGMENTS

The authors would like to thank M.E.Rensink for his help with grid generation in UEDGE, and L.L.LoDestro for many critical comments on the manuscript. This work was performed for U.S. Department of Energy by Lawrence Livermore National Laboratory under Contract DE-AC52-07NA27344, and General Atomics under Contract DE-FG02-95ER54309.

VIII. APPENDIX: PARAMETER FILE

An example INGRID parameter file is shown below. In the file, the user is supposed to provide settings relevant to grid and Patch generation: 1) For the magnetic field geometry, the name (with path) of data file, in the commonly used neqdsk format; 2) For radial boundaries, the values of the normalized poloidal flux Ψ for each of the radial boundaries; 3) For poloidal boundaries, the code has options to use one of these: a) limiter data embedded in the eqdsk file b) limiter data provided in a separate file (the file name and path must be included) c) target plates geometry in separate files, one per each plate (the file names and paths must be included); 4) How many X-points to include in the domain, 1 or 2; 5) Approximate R,Z coordinates for each of the included X-points and for the magnetic axis, to provide initial guess for the solver; 6) Dimensions of sub-grids; 7) Options related to grid customization; 8) Options related to integrator settings.

```
# -----
# User data directories
```

```

# -----
dir_settings:
  eqdsk: ../data/SNL/DIII-D/ # dir containing eqdsk
  limiter: . # dir containing limiter
  patch_data: ../data/SNL/DIII-D/ # dir containing patch data
  target_plates: ../data/SNL/DIII-D/ # dir containing target plates
# -----
# eqdsk file name
# -----
eqdsk: neqdsk
# -----
# General grid settings
# -----
grid_settings:
# -----
# Settings for grid generation
# (num cells, transforms, distortion_correction)
# -----
grid_generation:
  distortion_correction:
    all:
      active: True # true, 1 also valid.
      resolution: 1000
      theta_max: 120.0
      theta_min: 80.0
  np_default: 3
  nr_default: 3
  poloidal_f_default: x, x
  radial_f_default: x, x
# -----

```

```

# guard cell size
# -----
guard_cell_eps: 0.001
# -----
# num levels in efit plot
# -----
nlevs: 30
# -----
# num xpts
# -----
num_xpt: 1
patch_generation:
  strike_pt_loc: target_plates # 'limiter' or 'target_plates'
  rmagx_shift: 0.0
  zmagx_shift: 0.0
# -----
# Psi levels
# -----
psi_1: 1.066
psi_core: 0.95
psi_pf_1: 0.975
# -----
# magx coordinates
# -----
rmagx: 1.75785604
zmagx: -0.0292478683
# -----
# xpt coordinates
# -----
rxpt: 1.300094032687

```

```
zxpt: -1.133159375302
# -----
# Filled contours vs contour lines
# -----
view_mode: filled
# -----
# Saved patch settings
# -----
patch_data:
  file: LSN_patches_1597099640.npy
  preferences:
    new_file: true
    new_fname: LSN_patches_1597099640.npy
    use_file: false
# -----
# Integrator
# -----
integrator_settings:
  dt: 0.01
  eps: 5.0e-06
  first_step: 5.0e-05
  max_step: 0.064
  step_ratio: 0.02
  tol: 0.005
# -----
# Limiter settings
# -----
limiter:
  file: ''
  use_efit_bounds: false
```

```

# -----
# target plate settings
# -----

target_plates:
  plate_E1:
    file: d3d_otp.txt
    zshift: -1.6
  plate_W1:
    file: d3d_itp.txt
    zshift: -1.6

```

Listing 1: The YAML formatted configuration file. YAML files utilize Python formatted comments, keyword-value mappings, and nesting of structures via indentation.

REFERENCES

- ¹M. Kotschenreuther, *Physics of Plasmas* **14**, 072502 (2007).
- ²D. D. Ryutov, *Physics of Plasmas* **14**, 064502 (2007).
- ³D. D. Ryutov, *Physics of Plasmas* **15**, 092501 (2008).
- ⁴B. LaBombard, *Nuclear Fusion* **55**, 053020 (2015).
- ⁵T. D. Rognlien, D. D. Ryutov, N. Mattor, and G. D. Porter, *Physics of Plasmas* **6**, 1851 (1999).
- ⁶S. Wiesen, *Journal of Nuclear Materials* **463**, 480 (2015).
- ⁷R. Simonini, *Journal of Nuclear Materials* **34**, 368 (1994).
- ⁸M. V. Umansky, M. S. Day, and T. D. Rognlien, *Numerical Heat Transfer, Part B* **47**, 533 (2005).
- ⁹R. Marchand and M. Dumberry, “CARRE: a quasi-orthogonal mesh generator for 2d edge plasma modelling,” *Computer Physics Communications* **96**, 232 – 246 (1996).
- ¹⁰A. Taroni, “The multi-fluid codes Edgeid and Edge2D: Models and results,” *Contribution to Plasma Physics* **34**, 448 (1992).
- ¹¹O. Izacard and M. Umansky, “Gingred, a general grid generator for 2d edge plasma modeling,” (2017), arXiv:1705.05717 [physics.plasm-ph].
- ¹²J. P. Freidberg, *Ideal MHD* (Cambridge University Press, New York, 2014).

- ¹³D. D. Ryutov, M. A. Makowski, and M. V. Umansky, “Local properties of the magnetic field in a snowflake divertor,” *Plasma Physics and Controlled Fusion* **52**, 105001 (2010).
- ¹⁴L. Lao, H. S. John, R. Stambaugh, A. Kellman, and W. Pfeiffer, “Reconstruction of current profile parameters and plasma shapes in tokamaks,” *Nuclear Fusion* **25**, 1611–1622 (1985).
- ¹⁵W. H. Press, S. A. Teukolsky, W. T. Vetterling, and B. P. Flannery, *Numerical Recipes in C*, 2nd ed. (Cambridge University Press, Cambridge, USA, 1992).
- ¹⁶P. Virtanen, R. Gommers, T. E. Oliphant, M. Haberland, T. Reddy, D. Cournapeau, E. Burovski, P. Peterson, W. Weckesser, J. Bright, S. J. van der Walt, M. Brett, J. Wilson, K. J. Millman, N. Mayorov, A. R. J. Nelson, E. Jones, R. Kern, E. Larson, C. Carey, İlhan Polat, Y. Feng, E. W. Moore, J. VanderPlas, D. Laxalde, J. Perktold, R. Cimrman, I. Henriksen, E. A. Quintero, C. R. Harris, A. M. Archibald, A. H. Ribeiro, F. Pedregosa, P. van Mulbregt, and S. . . Contributors, “Scipy 1.0—fundamental algorithms for scientific computing in python,” (2019), arXiv:1907.10121 [cs.MS].
- ¹⁷I. Enthouart, “SciPy Interpolate GitHub repository,” <https://github.com/scipy/scipy/tree/master/scipy/interpolate>.
- ¹⁸“scipy.optimize.root documentation,” <https://docs.scipy.org/doc/scipy/reference/generated/scipy.optimize.root.html>.
- ¹⁹A. Hindmarsh, “Odepack. a collection of ode system solvers,” (1992).
- ²⁰O. Meneghini, S. Smith, L. Lao, O. Izacard, Q. Ren, J. Park, J. Candy, Z. Wang, C. Luna, V. Izzo, B. Grierson, P. Snyder, C. Holland, J. Penna, G. Lu, P. Raum, A. McCubbin, D. Orlov, E. Belli, N. Ferraro, R. Prater, T. Osborne, A. Turnbull, and G. Staebler, “Integrated modeling applications for tokamak experiments with OMFIT,” *Nuclear Fusion* **55**, 083008 (2015).
- ²¹O. Meneghini and L. Lao, “Integrated modeling of tokamak experiments with omfit,” *Plasma and Fusion Research* **8**, 2403009–2403009 (2013).
- ²²“UEDGE code GitHub repository,” <https://github.com/LLNL/UEDGE>, accessed: 2021-01-18.
- ²³K. Simonov, “Pyyaml homepage,” <https://pyyaml.org/wiki/PyYAML> (2006).
- ²⁴M. E. Rensink and T. D. Rognlien, “Mapping of orthogonal 2d flux coordinates for two nearby magnetic x-points to logically rectangular domains,” Tech. Rep. LLNL-TR-731515 (Lawrence Livermore National Laboratory, Livermore, California, 2017).
- ²⁵B. M. Garcia, J. Watkins, J. Guterl, and M. V. Umansky, “INGRID code GitHub repository,” <https://github.com/LLNL/INGRID> (2019).
- ²⁶B. M. Garcia, J. Watkins, J. Guterl, and M. V. Umansky, “INGRID Read the Docs,” <https://github.com/LLNL/INGRID>

//ingrid.readthedocs.io/en/latest/ (2020).

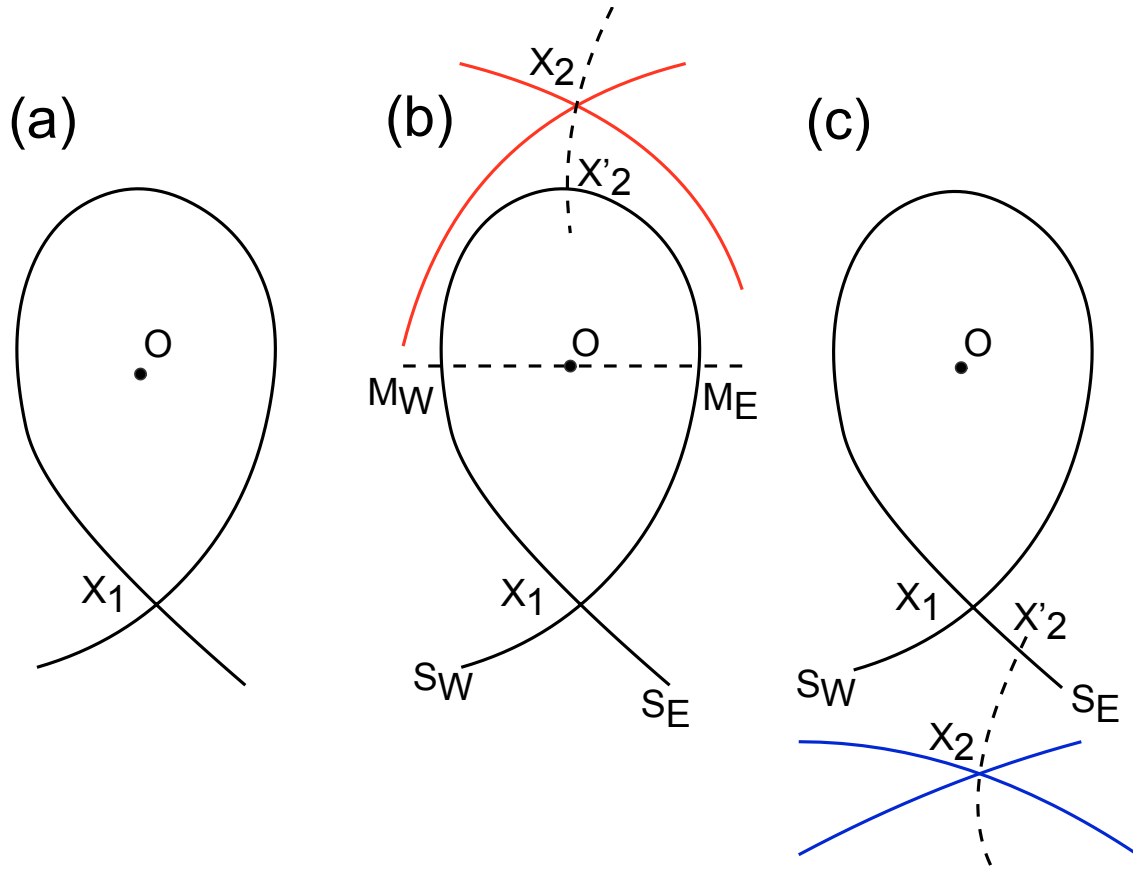


Figure 1: Topological possibilities with one and two X-points. As explained in the main text, case (a) is a single-null configuration; case (b) with the secondary X-point in the common-flux region has five variations, depending on the location of the projection point X'_2 ; case (c) with the secondary X-point in the private-flux region has two variations depending on the location of the projection point X'_2 . The East-West notation for the two midplane points and the two strike points is based on designating the direction from the primary X-point toward the O-point as “North”. This is invariant notation, independent on whether the primary X-point is at the top, at the bottom, or anywhere else.

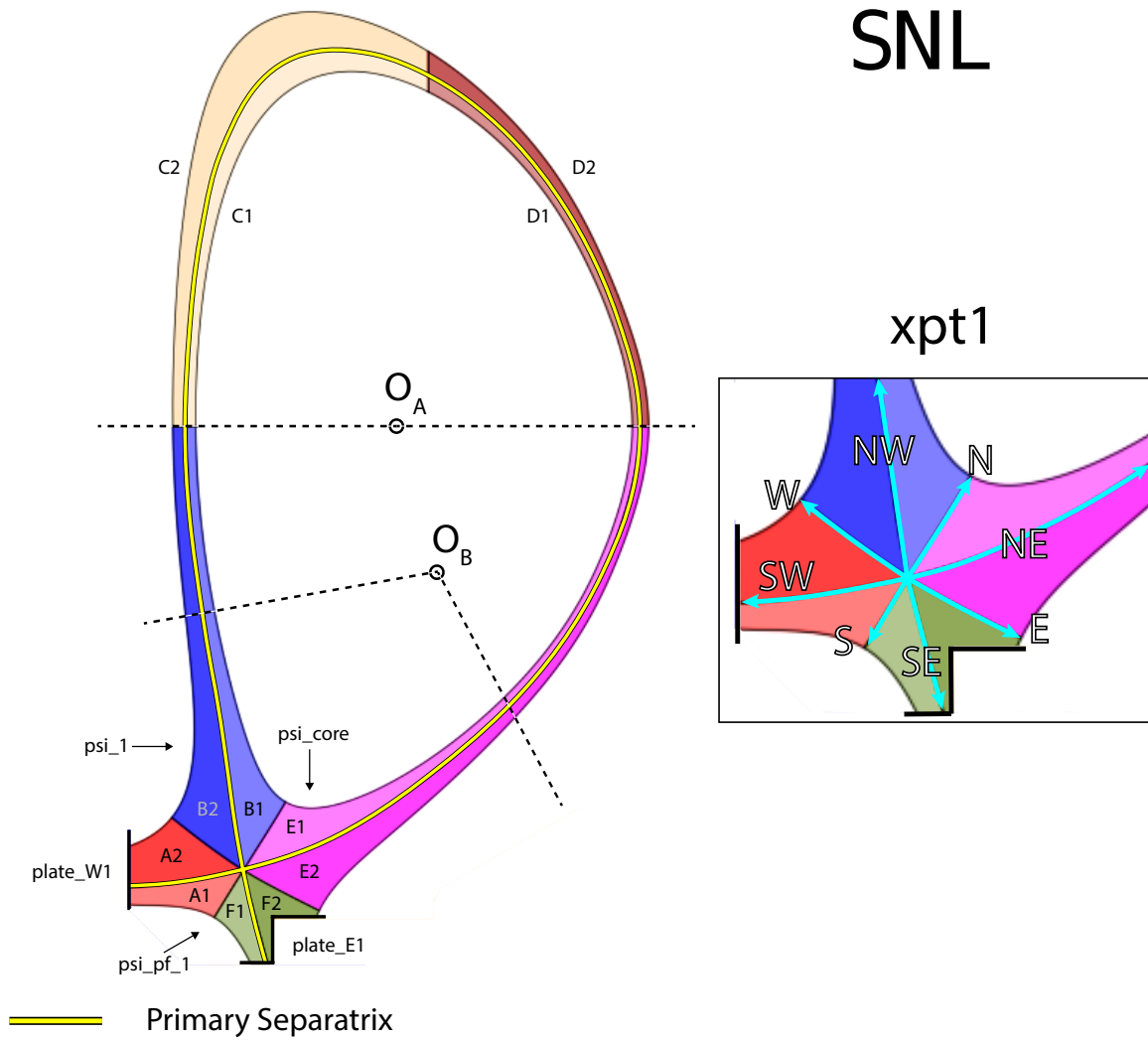
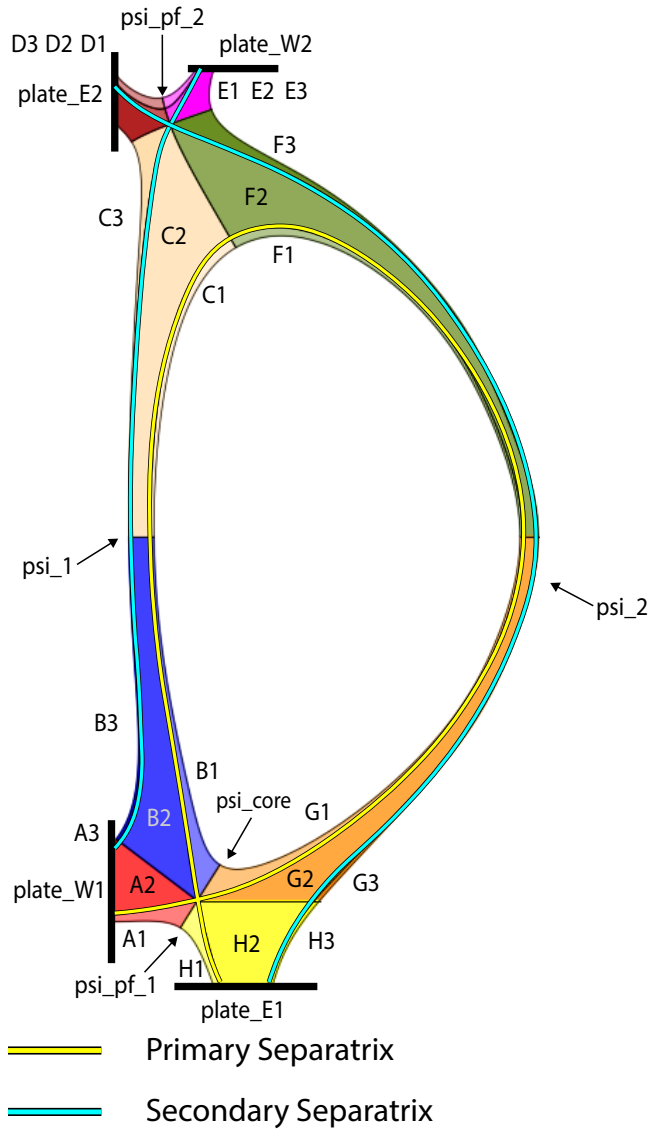
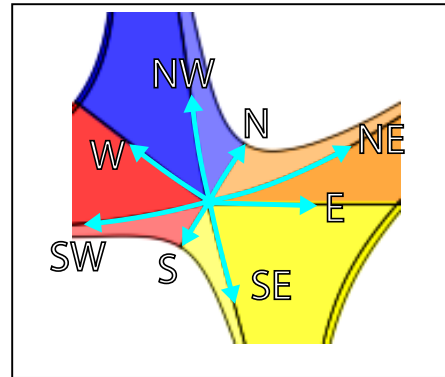


Figure 2: SNL Patch-Map with the generalized midplane overlaid. O_A shows the original magnetic axis used to define the horizontal midplane through O_A . The midplane defines the poloidal boundary between patches B/C and D/E. For Patch map customizability, INGRID allows for a generalized midplane through O_B to be defined (described in Section II-G). This is done by redefining the location of the magnetic axis and the directions of the rays generating the midplane.



UDN

xpt1



xpt2

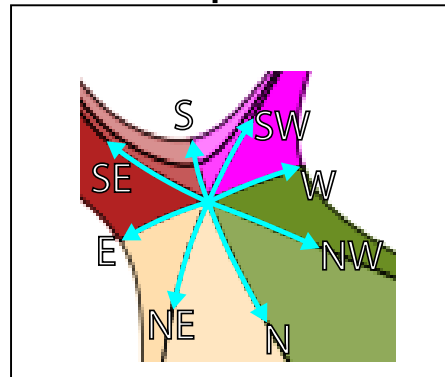


Figure 3: UDN Patch-Map

SF15

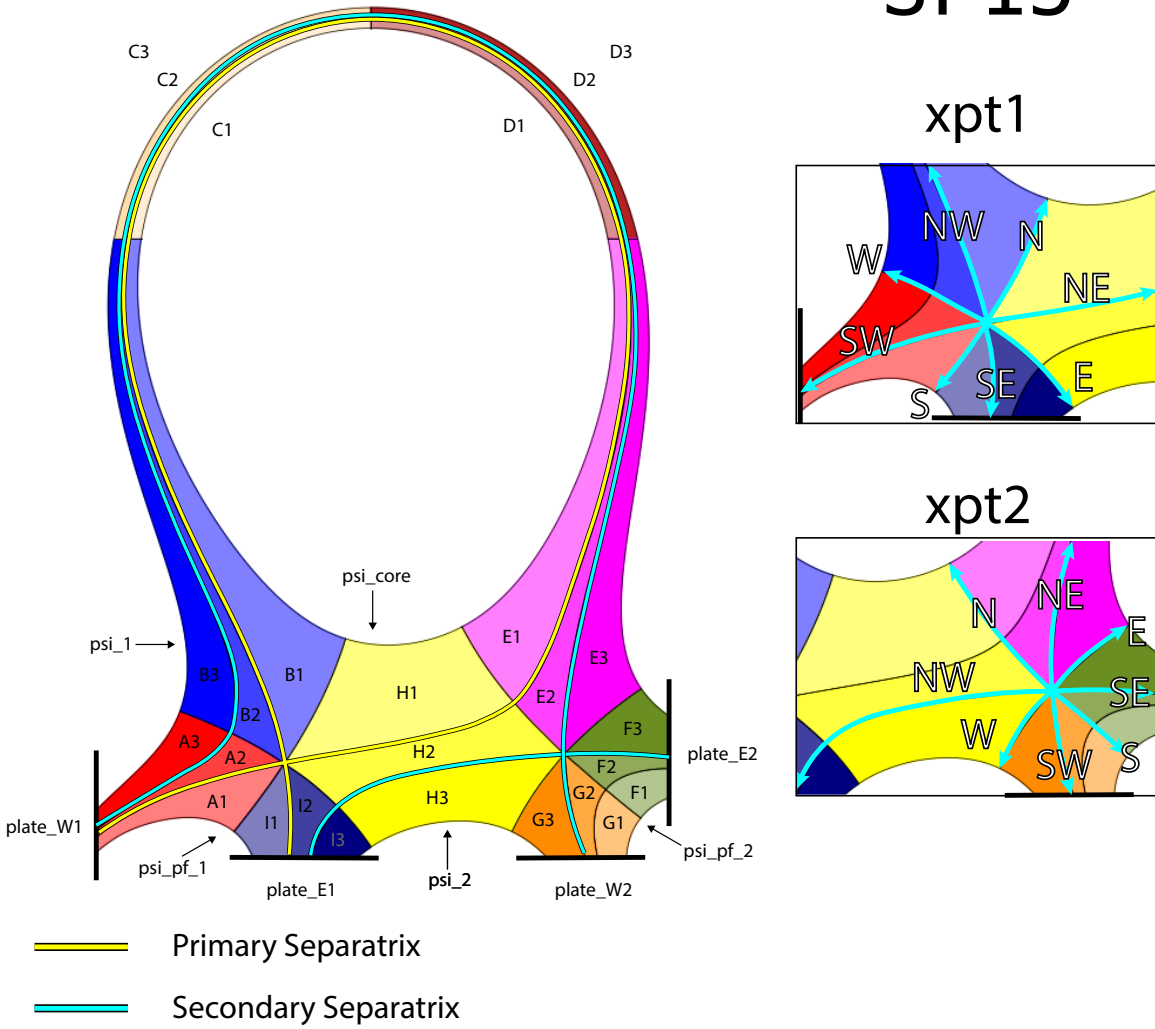


Figure 4: SF15 Patch-Map

SF45

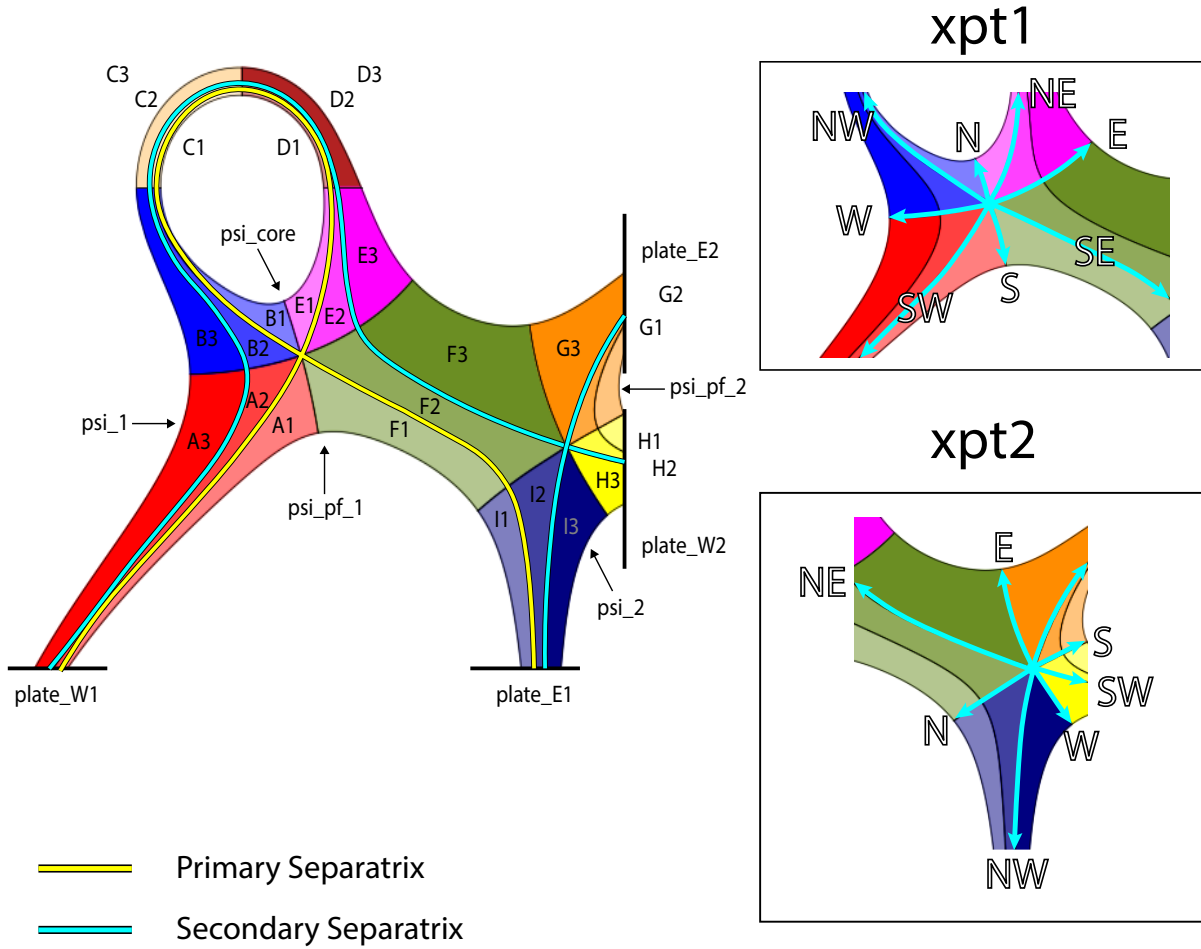


Figure 5: SF45 Patch-Map

SF75

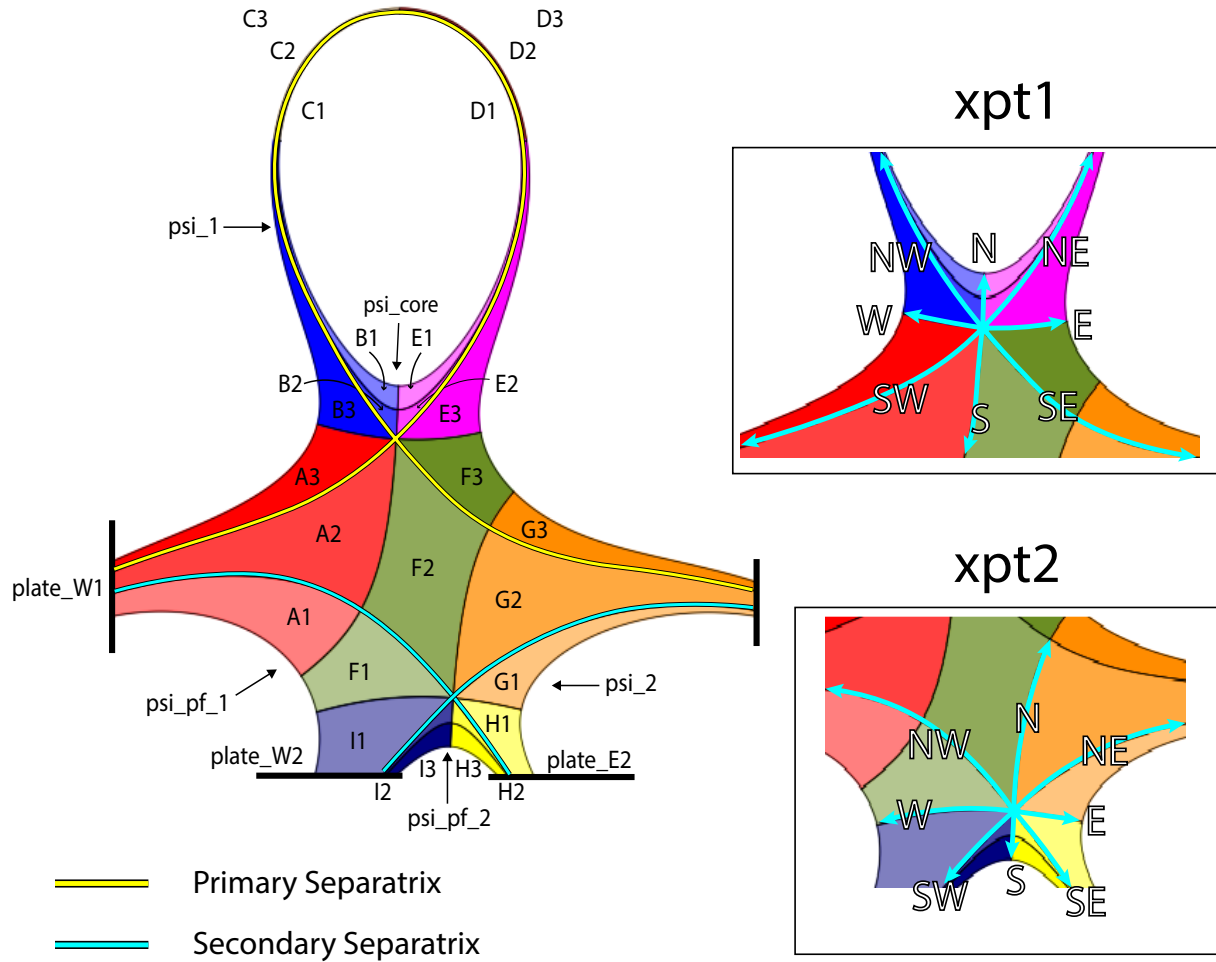


Figure 6: SF75 Patch-Map

SF105

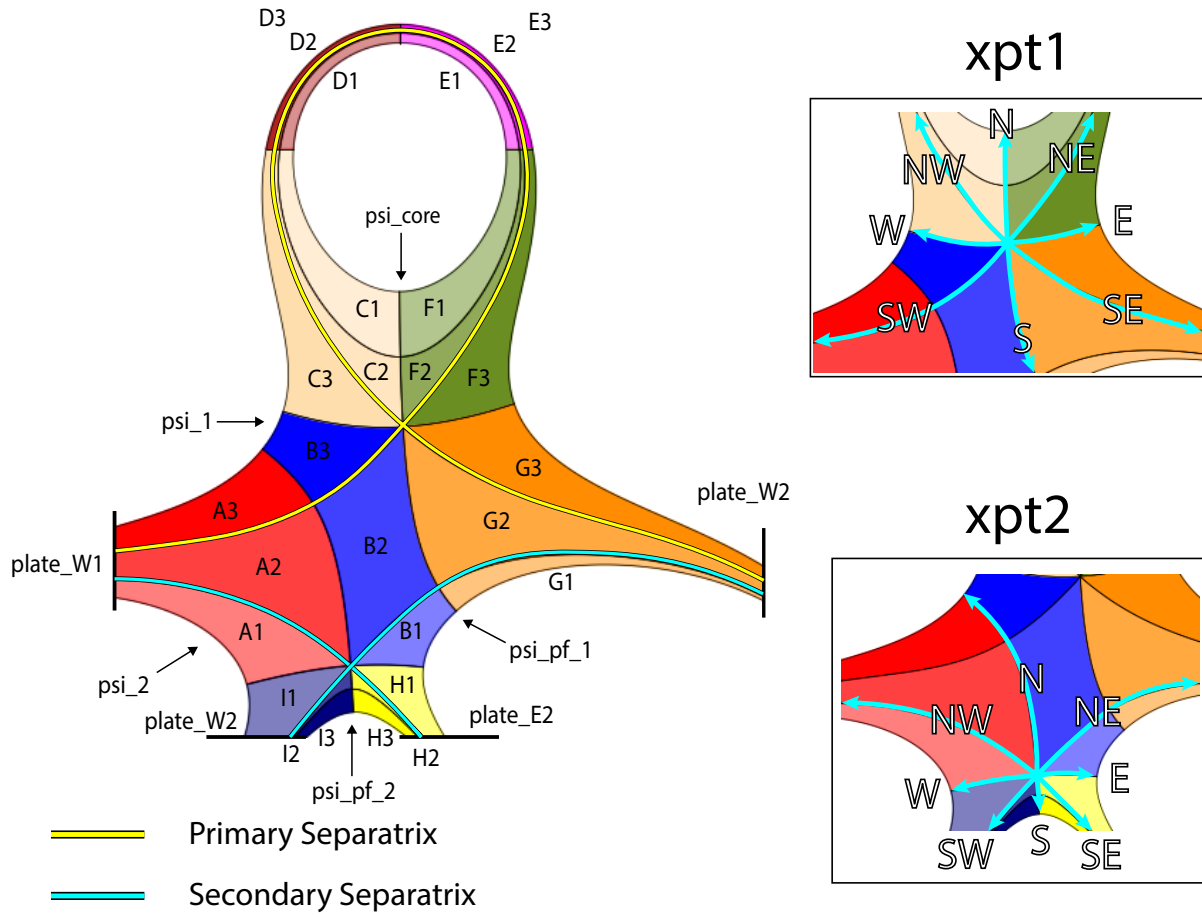


Figure 7: SF105 Patch-Map

SF135

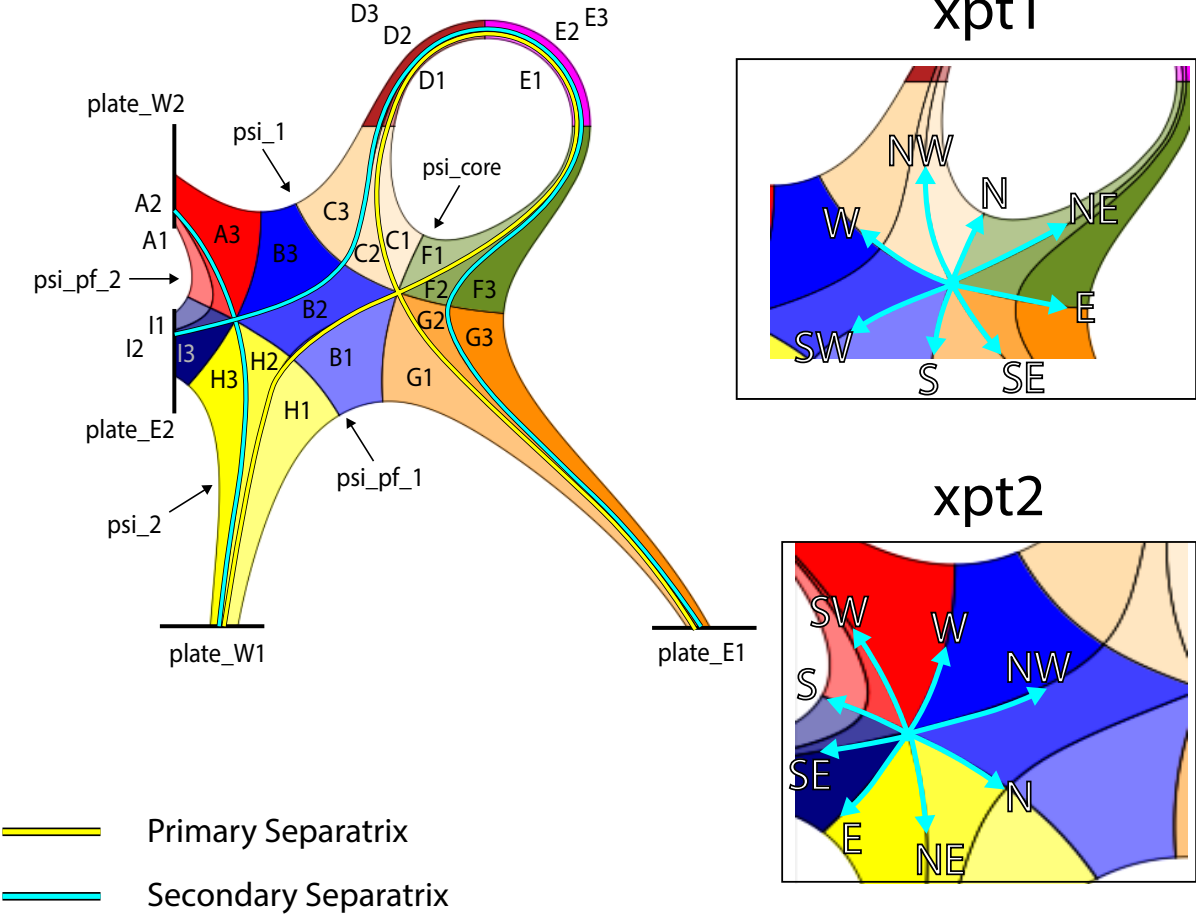
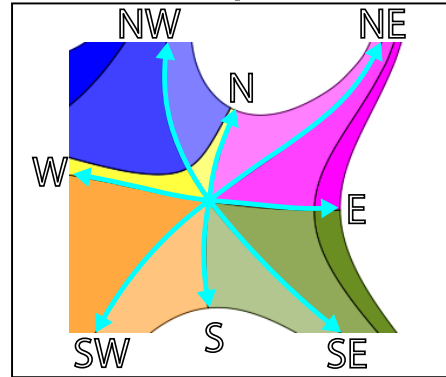


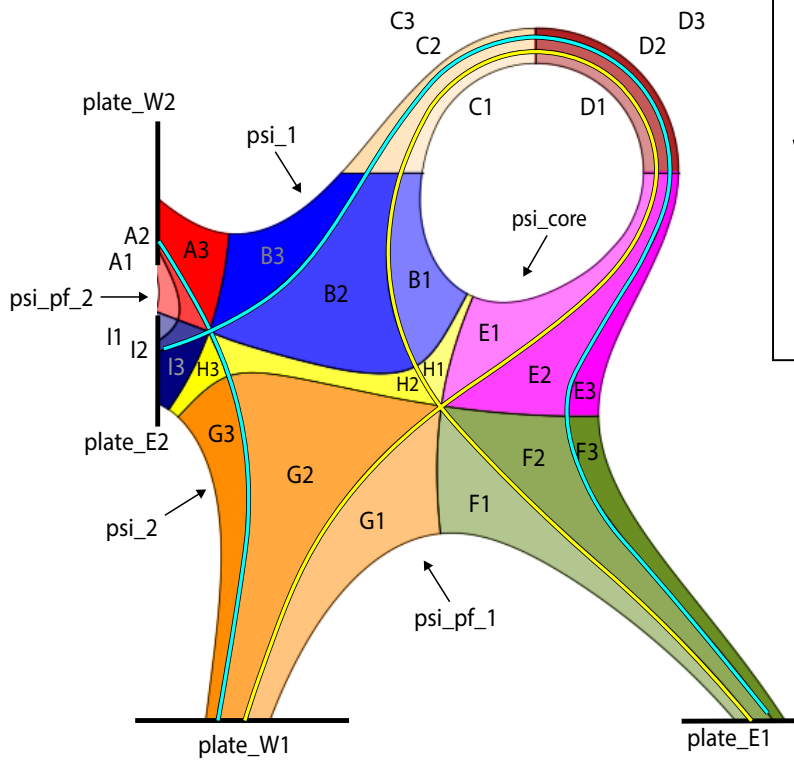
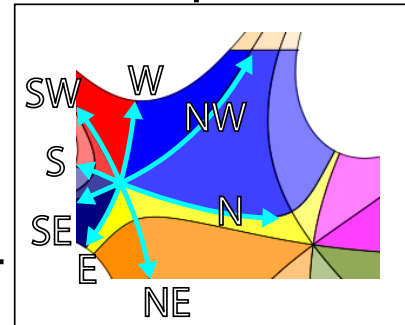
Figure 8: SF135 Patch-Map

SF165

xpt1



xpt2



- Primary Separatrix
- Secondary Separatrix

Figure 9: SF165 Patch-Map

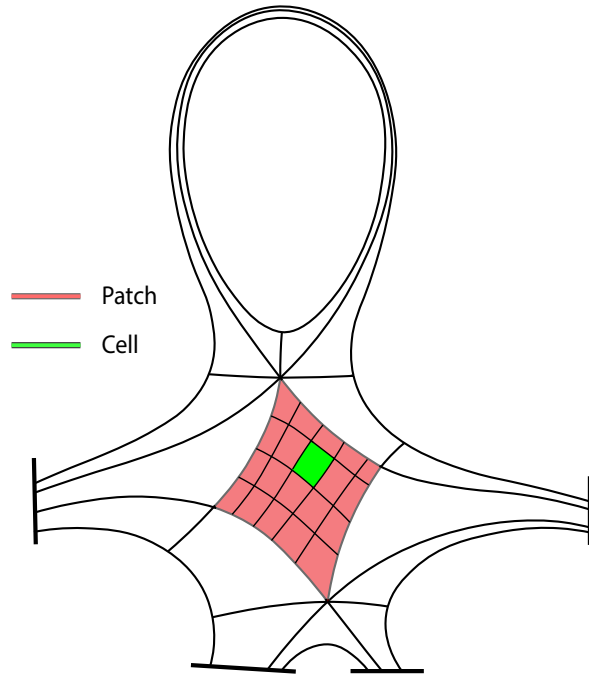


Figure 10: INGRID Patch-Map; a subgrid is shown on one of the patches

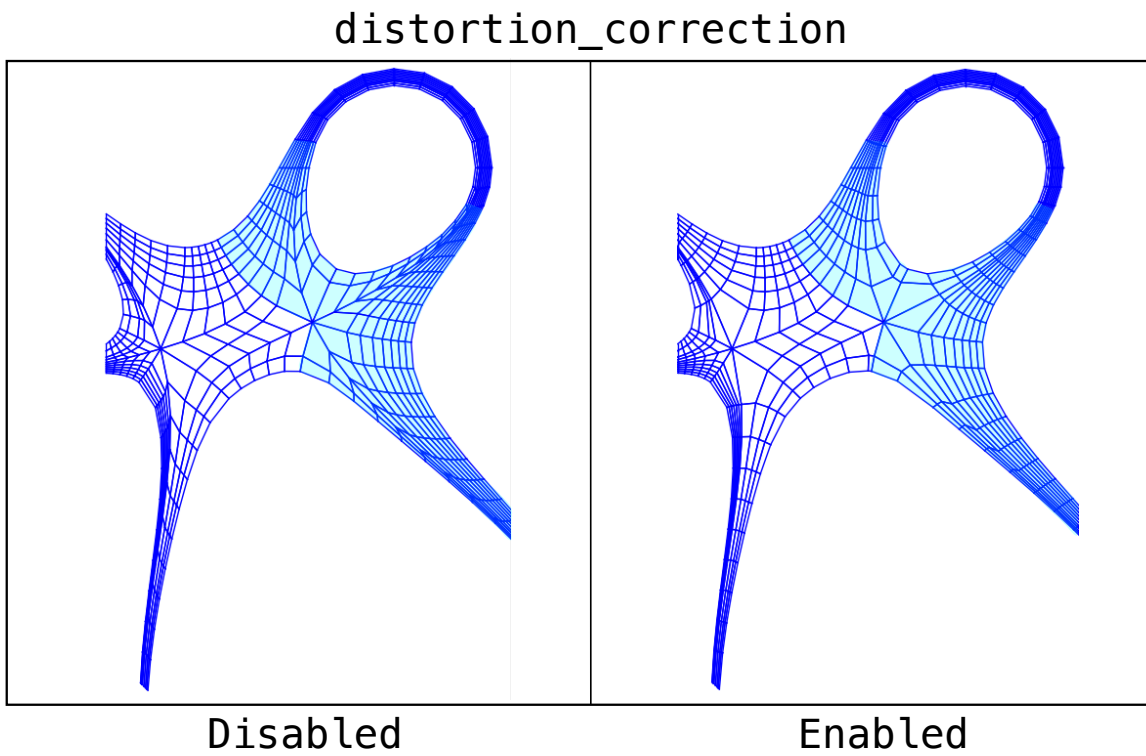


Figure 11: Comparison of SF135 grids generated with and without activation of the distortion_correction tool. Highlighted regions illustrate regions of notably improved grid orthogonality.

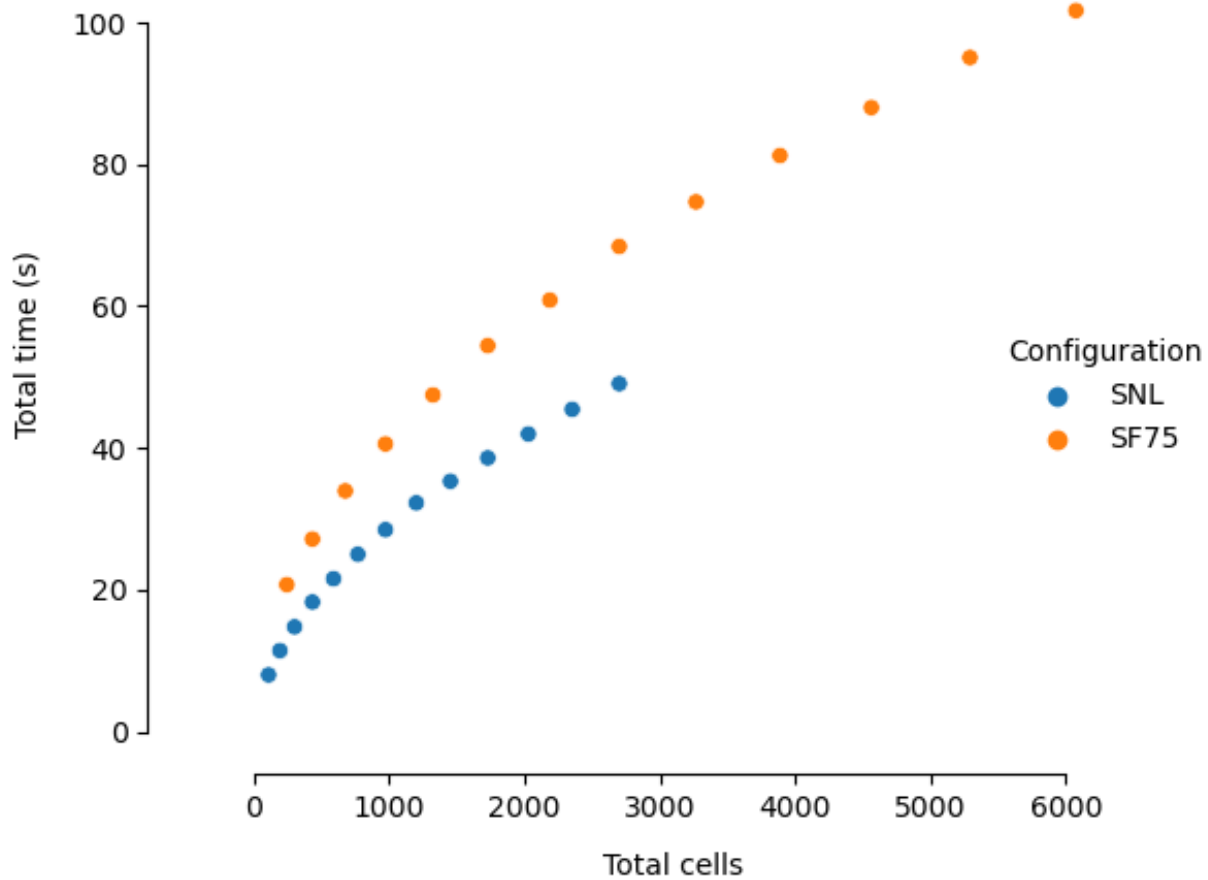


Figure 12: Scaling of grid generation follows a sublinear trend independent of configuration. Grids were generated with $n \times n$ many cells per Patch with $n = \{3, 4, 5, \dots, 15\}$. With $n \times n$ subgrid dimensions, SNL configurations contain $12n^2$ many cells, whereas SF75 configurations contain $27n^2$ many cells.

INGRID

UEDGE

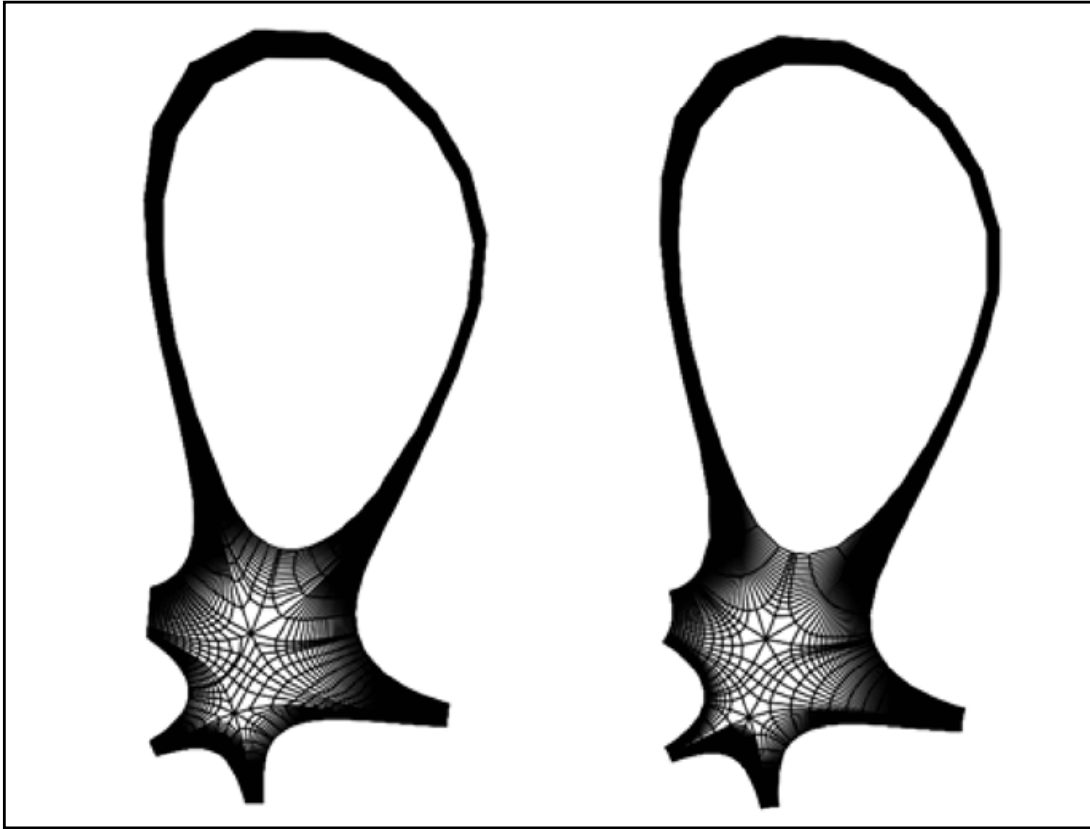


Figure 13: INGRID and UEDGE generated grids used for the benchmark calculations.

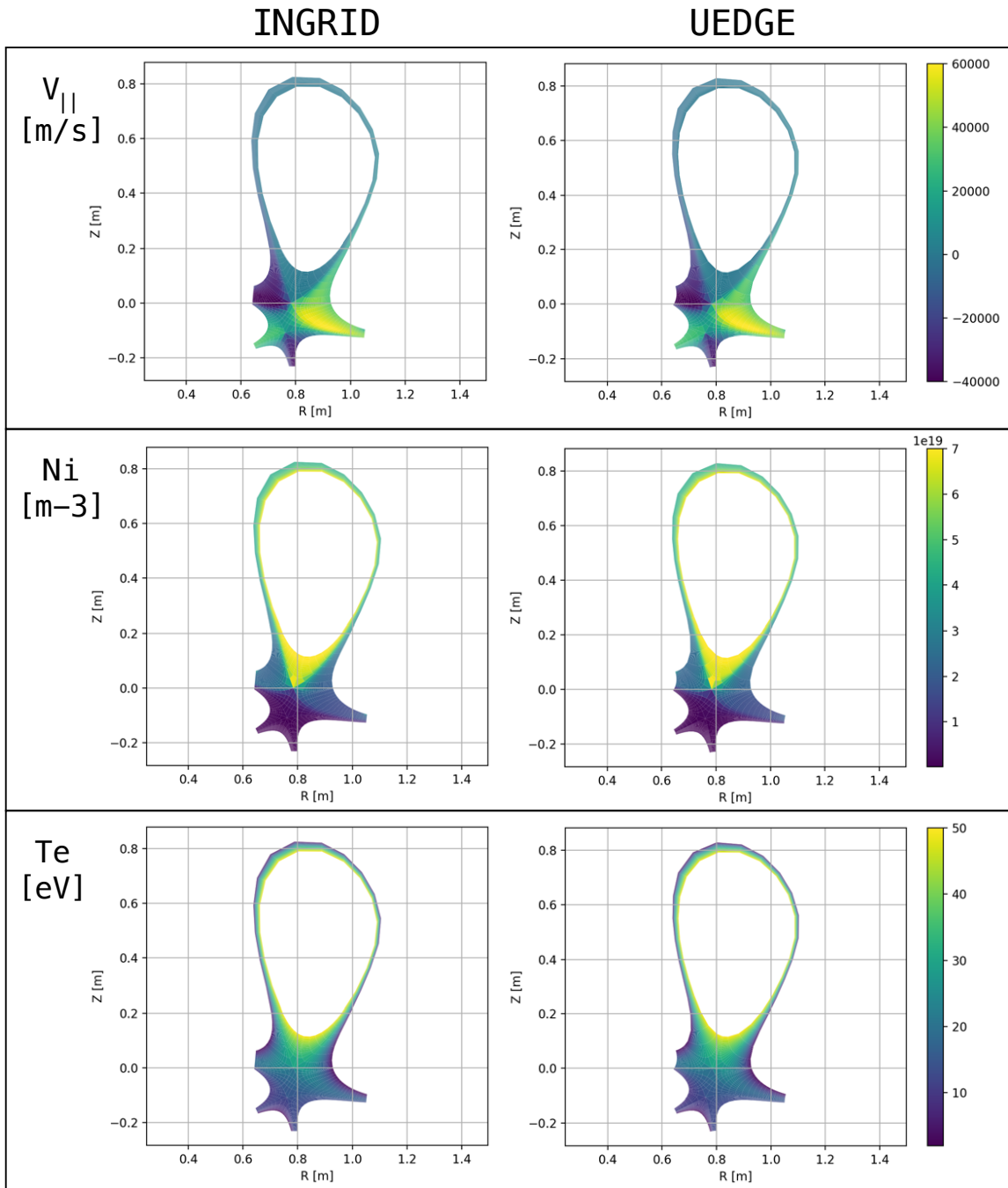


Figure 14: Results of the benchmark calculations run on INGRID and UEDGE generated grids.

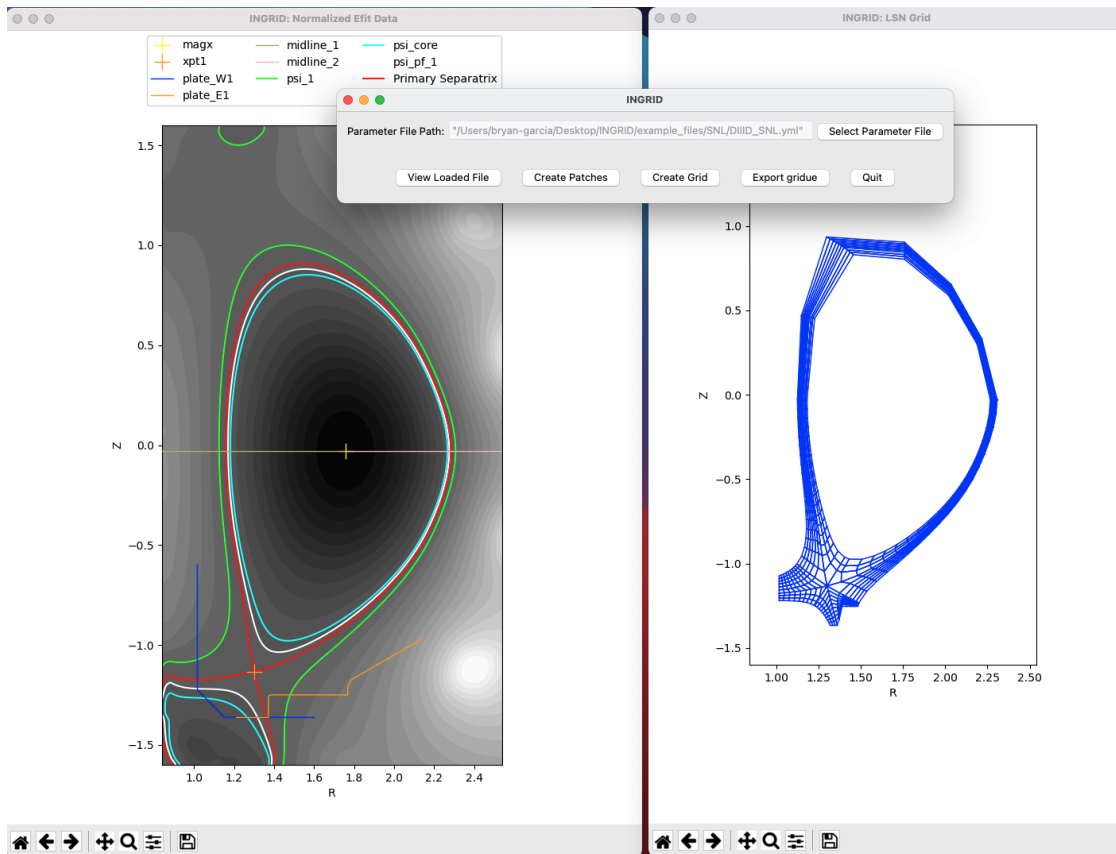


Figure 15: The INGRID GUI with loaded EFIT data and an INGRID generated grid plotted in separate windows. This interface allows users to load a parameter file, plot the contents, create a Patch map, create a grid, and export a gridue.